Event-based collapse fragility development of electrical transmission towers for regional hurricane risk analysis

Xinlong Du[1] and Jerome F. Hajjar[2]

[1]Graduate Research Assistant, Department of Civil and Environmental Engineering, Northeastern University, Boston, MA 02115, USA. Email: du.xinl@northeastern.edu

[2]CDM Smith Professor and Chair, Department of Civil and Environmental Engineering, Northeastern University, Boston, MA 02115, USA. Email: jf.hajjar@northeastern.edu

ABSTRACT

In the United States, blackouts during hurricanes may be caused by collapse of electrical transmission towers. Fragility curves that document the likelihood of collapse of these towers are needed for fast damage assessment and emergency management of electrical transmission networks. This paper introduces a methodology for developing event-based fragility curves that relate the collapse probability of a transmission tower after a hurricane event to the hurricane intensity measure. The intensity measure of a hurricane is the storm-maximum gust wind speed at 10 m height. The fragility curve is the cumulative distribution function of the collapse capacity, which is a random variable defined as the intensity measure associated with the onset of collapse. Incremental dynamic analysis (IDA) is used along with a suite of selected hurricane wind records to model collapse and to propagate uncertainties from hurricane wind speeds, directions, and durations to the collapse capacity. To save computational resources, IDA can be run up to a certain moderate intensity level instead of collapse of a structure. This is called a truncated IDA, where some IDA curves may only provide a lower bound value of the collapse capacity. The collapse capacity is assumed to follow a lognormal distribution, whose parameters are estimated with the method of moments or the maximum likelihood method for the traditional IDA or truncated IDA, respectively. To facilitate regional damage assessment, the region of interest is discretized into a set of grids and a set of fragility curves are developed for each grid considering the variations in selected hurricane wind records and tower orientations. This procedure is demonstrated using Massachusetts as a testbed. Even though transmission towers are only considered in this paper, the event-based fragility methodology can be adopted to buildings or other structures subjected to hurricanes.

Keywords: event-based fragility, collapse, transmission tower, hurricane, regional analysis, incremental dynamic analysis

1. Introduction

In electrical transmission systems, lattice towers are widely used to support overhead conductors. These towers are exposed and vulnerable to windstorms such as hurricanes. For example, Hurricane Katrina in 2005 led to 402 cable support towers in Mississippi damaged or collapsed [1], and Hurricane Harvey in 2017 damaged or collapsed more than 850 transmission structures [2]. The constantly emerging evidence of collapse of transmission towers under hurricanes shows the necessity for capacity assessment of these structures considering geometric and material nonlinearities. To quantitatively assess the vulnerability of electrical transmission towers subjected to windstorms, both empirical [3, 4] and analytical [5-10] fragility curves have been adopted by researchers. In addition, as structural engineers are moving towards performance-based wind design, geometric nonlinear and inelastic deformations are allowed but should be controlled under strong winds [11]. Therefore, nonlinear analysis will be increasingly important in wind design and capacity assessment of buildings and other structures. This paper focuses on collapse fragility development of electrical transmission towers considering nonlinear and dynamic effects.

Fragility curves are used to describe the relationship between the failure probability of a structure and the intensity measure of the applied hazard. To calculate the failure probability of a structure for a certain intensity level of hazard is a standard structural reliability problem, where the uncertainties may come from structural properties and hazards with the same intensity level but other different characteristics. Therefore, each point on a fragility curve can be obtained from a structural reliability analysis. Depending on the uncertainties considered in the limit state function, there are time-invariant reliability and time-variant reliability. Consequently, fragility curves can also be developed based on time-invariant reliability or time-variant reliability.

For the time-invariant reliability approach, the limit state function can be expressed as $g(\boldsymbol{X})$, where $\boldsymbol{X}$ is a set of random variables. The fragility is defined as the failure probability of the structural system conditional on the specified intensity measure IM, i.e., $P(g(\boldsymbol{X}) \leq 0|IM)$. To satisfy the precondition of time-invariant reliability, one should assume the loads are static or consider the dynamic effects implicitly through some amplification factors. For example, Ellingwood et al. [12] and Li [13] developed hurricane fragility curves for light-frame wood construction using design equations with static wind pressure and a gust-effect factor to account for the maximum dynamic response. The conditional failure probabilities that form the fragility curves were obtained by increasing the wind speed in 10 mph increments and repeating the first-order reliability method (FORM) at each increment. The results were also used to validate the two-parameter lognormal cumulative distribution function (CDF) model of fragility curves by a series of statistical analyses [13, 14], which shows that the lognormal CDF provides a good model for fragility curves of light-frame wood construction. Shanmugam [15] also developed fragility curves for roof uplift capacities in low-rise residential construction by using static wind loads, but considered correlated non-normal random variables. Shanmugam [15] accepted the idea that the fragility can be modeled as a lognormal CDF, so she did not use FORM or any other reliability methods to calculate failure probabilities, but combined Monte Carlo simulation and the maximum likelihood method suggested by Shinozuka et al. [16] to estimate the two parameters of the lognormal CDF. Similarly, Shafieezadeh et al. [17] and Darestani et al. [9] assumed static wind loads with gust-effect factors according to ASCE 7 [18, 19] and developed fragility curves for utility wood poles and transmission towers, respectively. However, the gust-effect factor is developed for structural design and assumes that the structure remains linear elastic. Therefore, the design equations with a gust-effect factor may not be used for highly nonlinear collapse failure analysis.

For the time-variant reliability approach, the failure event is described with respect to a time domain. For example, a time-variant reliability problem may be defined with a limit state function $g(\boldsymbol{X}, \boldsymbol{Y}(t))$, where $\boldsymbol{Y}(t)$ represents a set of random processes such as time histories of wind speeds and ground motions. For a certain time t, $\boldsymbol{Y}(t)$ becomes a set of random variables; therefore, the instantaneous failure probability at time *t* may be obtained through the approaches for calculating time-invariant reliabilities. Traditionally, the failure probability is asked to be estimated in a time interval, which is the first-passage problem and can be solved by using a series system approximation after discretizing the time interval or estimating the mean rate of down-crossings of the random process $g(\boldsymbol{X}, \boldsymbol{Y}(t))$ below zero [20]. A more practical time-variant reliability problem may be defined by a limit state function $g(\boldsymbol{X}, \boldsymbol{Y}(0) \sim \boldsymbol{Y}(t))$, which means that the instantaneous failure event at time *t* depends on the random processes $\boldsymbol{Y}(t)$ from time 0 to *t*. For example, due to the dynamic effects and plastic deformations, the structure's response at time *t* dependents on the force time history from 0 to *t*; thus, the failure probability at time *t* dependents on the force time history from 0 to *t*. Similar methods may be used to solve the problem as was done for the limit state function $g(\boldsymbol{X}, \boldsymbol{Y}(t))$. However, the correlations of failures between different time points needs to be considered [20-23]. For the limit state function $g(\boldsymbol{X},\ \boldsymbol{Y}(0) \sim \boldsymbol{Y}(t))$, if only the failure probability after an event (i.e., at the end of the loading time history) is of interest, Monte Carlo simulation may be used to account for the uncertainties from random processes $\boldsymbol{Y}(t)$. For fragility development, a set of time history analyses may be run using different $\boldsymbol{Y}(t)$'s to propagate the uncertainties from $\boldsymbol{Y}(t)$ to structural responses. In this paper, fragilities developed through this way are called event-based fragilities. Event-based fragilities are widely used in earthquake engineering, where the failure probability provided by fragility curves is for a seismic event, and fragility curves are usually developed using nonlinear dynamic analysis with a suite of ground motions. However, event-based fragilities have not been introduced into wind engineering for windstorm events such as hurricanes and tornados.

In the context of fragility development for transmission towers under wind loads, researchers attempted to develop analytical fragility curves using static analysis [5, 9] or dynamic analysis with fixed time intervals such as 2 minutes [8, 10], 5 minutes [6], and 10 minutes [7]. The fragilities developed for these time intervals cannot represent the fragilities for a whole windstorm event because wind speeds and directions may vary during a storm, and failure of a structure incorporates accumulating phenomena such as yielding and dynamic effects. When using these fragility curves, the duration of a windstorm is discretized into a series of short time intervals (e.g., 2 minutes), and the failure probability is calculated for each time interval independently. However, as discussed before the failure probabilities within those short time intervals are correlated [20, 24]. This correlation is difficult to quantify from the view of time-variant reliability and is not considered by the above authors. Hallowell et al. [25] used the 1-hour peak wind record to represent a whole hurricane and tried to develop fragility curves for a hurricane event. For this case, except for the problem that the structure may be damaged before the 1-hour peak wind record, another problem here is that the 1-hour peak wind record is not necessarily the worst hour within a storm. For example, for a transmission tower the wind direction of the 1-hour peak wind record may be parallel to conductors and thus the wind forces on conductors may be negligible, while there may be a worse hour which has a lower wind speed but a wind direction perpendicular to the conductors.

To overcome the above-mentioned limitations of the current fragility development strategies for wind loads, this research applies the event-based fragility for windstorms and focuses on collapse of transmission towers subjected to hurricanes. The limit state function has a form of $g(\boldsymbol{X},\ \boldsymbol{Y}(0) \sim \boldsymbol{Y}(t))$ since nonlinear and dynamic effects are included in collapse modeling. Instead of assessing failure probabilities for a series of time intervals within a hurricane, the event-based fragility tries to estimate the failure probability after a hurricane event so that users can avoid the intractable task of quantifying correlations of failure probabilities in different time intervals. The storm-maximum 3-second gust wind speed is adopted as the intensity measure of hurricanes, and a suite of hurricane wind speed and direction records are selected to represent the uncertainties in wind loading [26]. The collapse limit state is considered through incremental dynamic analysis (IDA) adapted from earthquake engineering [27], from which the collapse capacity (i.e., the intensity measure associated with the onset of collapse) is obtained. The parameter estimation approaches for fragility curves are introduced for cases that the collapse capacity points for all wind records are completely or partially captured on IDA curves. Finally, a methodology is proposed for developing collapse fragility curves for transmission towers in a region using its specific towers and hurricane wind records.

2. Uncertainties in hurricane wind records

It is well-known that hurricane wind records with the same intensity measure may have different patterns or uncertainties in terms of the changing of wind speeds and directions. In fragility analysis, these uncertainties should be modeled and propagated to structural responses. For event-based fragilities, the record-to-record uncertainties can be considered through Monte Carlo simulation, which requires running IDAs for a suite of hurricane wind records collected for a location of interest. To achieve this goal, Du et al. [26] used Massachusetts as a testbed, discretized it into a series of grids (Fig. 1), and collected hurricanes wind records for each grid from a 10,000-year synthetic hurricane catalog [28]. However, due to the high computational demand, it is intractable to use all the collected wind records (about 200 for each grid, each of which has a duration on the order of 10 hours) for IDAs and fragility development. A subset of the collected records is used in this work, while still preserving the key uncertainties in the loading. This is achieved through clustering of the wind records and selecting several of them from each cluster. Using a neural network autoencoder, Du et al. [26] first compressed the high-dimensional wind records into low dimensional latent features through a encoder process. The latent features were then expanded to reconstruct the wind records through a decoder process. Training of this neural network was done to minimize the difference between the original and the reconstructed wind records. Consequently, the low-dimensional latent features contain the most important information in the wind records. Finally, a k-means clustering algorithm was used on the latent features, through which approximately 1/10 of the wind records were selected in each cluster for fragility development. As such, the number of wind records used to run IDAs for each grid is approximately 20. As an example, 16 selected hurricane wind records from 8 clusters are shown in Fig. 2 for Grid 86 whose centroid has a latitude of 41.7 and a longitude of -70.1. Here the wind velocities are resolved into the North and East directions because the wind records have changing wind directions. Specifically, the wind records are time series of wind velocity vectors in 2D with a 10-min time step. Therefore, the clustering and selection process considers the effects of wind durations, speeds, and directions, which are all reflected in the values of the latent features. In Fig. 2, the wind records selected from the same cluster are shown in the same color, and it is seen that wind records within the same cluster have similar characteristics in terms of wind speeds, directions, and durations. In addition, 1-hour ramp-up and ramp-down loading histories are added to the beginning and the end, respectively, of each wind record to avoid an impulse effect due to sudden loading (see Fig. 2) for the nonlinear structural dynamic analyses in the following sections [11]. To better compare wind records from different clusters, wind records in Fig. 2 are put together with their midpoint of the duration occurring at the same time. To facilitate the autoencoder, zero paddings at the beginning and end of each record are used to make all records have the same duration in these plots; however, these zero paddings are removed in the following nonlinear dynamic analysis.

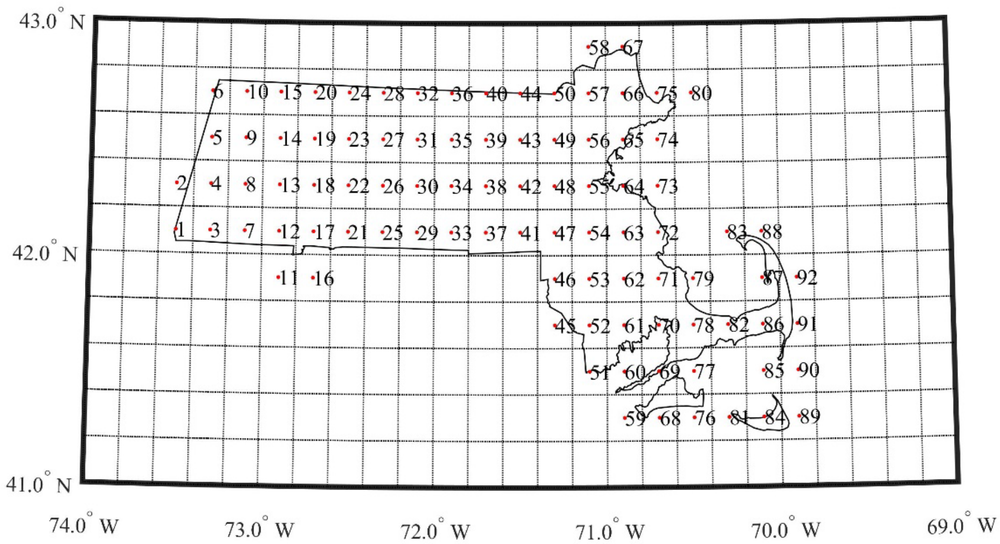

Fig. 1. Massachusetts is discretized into grids with their centroids shown and labelled

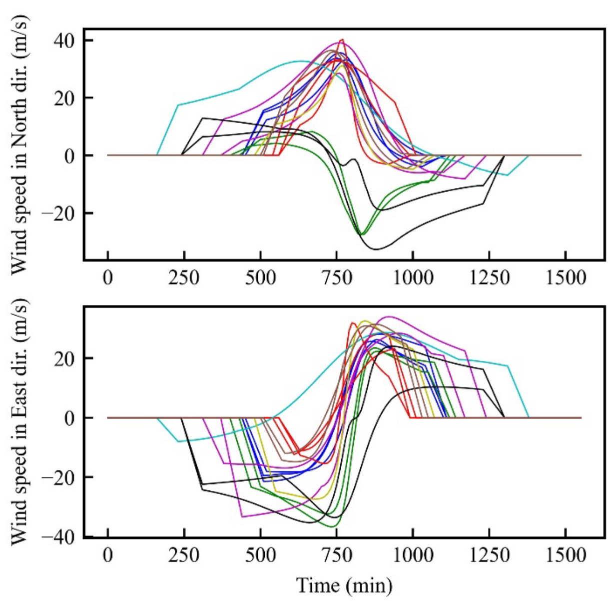

Fig. 2. An example of selected hurricane wind records for a grid

3. Hurricane wind loading on transmission towers

The selected hurricane wind records are 10-min mean wind speeds at 10 m height. To calculate the wind loads on transmission towers, the wind field along the towers should be generated, which includes modeling of the atmospheric boundary layer and the fluctuating wind speeds. The wind loading time histories may then be calculated based on the equations in the ASCE 74 design code [29].

3.1. Wind field simulation

As an example, Fig. 3 shows the step plot of a 10-min mean wind speed record at a 10 m height, along with the corresponding wind direction record. Note that the wind direction is clockwise positive from the North direction. Based on the 10-min mean wind speeds at 10 m height, the 10-min mean wind speeds at other heights along the tower are calculated according to the logarithmic law boundary layer model [30-32], which is

$$U(z) = \frac{u_*}{k} \ln \frac{z}{z_0} \tag{1}$$

where $U(z)$ is the mean wind speed at the height of z; u_* is the shear velocity; $k = 0.4$ is the Von Karman constant; z_0 is the roughness length of the ground surface. In this research, open terrain with a roughness length $z_0 = 0.03$ is assumed. After generating 10-min mean wind speeds for different heights, the fluctuating wind speeds should be superimposed to the mean wind speeds. Here the spatially correlated fluctuating wind speeds are simulated from the Kaimal spectrum [33] using the spectral representation method [34-36]. The correlations of fluctuating wind speeds at different locations are considered through a coherence function, which is an exponential decay as proposed by Davenport [37]. Fig. 4 presents the simulated and target spectra of the fluctuating wind speeds with a good match. The simulation of the fluctuating wind speeds is based on the open-source code developed by Cheynet [38]. After combining the mean and fluctuating wind speeds at different heights, the temporal-spatial evolution of the hurricane wind field along a transmission tower is obtained as presented in Fig. 5. Only the absolute values of the wind speeds are shown in Fig. 5, while the changing of the wind directions are omitted for simplicity of the figure. Note that within each 10-min time interval, the wind direction is assumed to be constant even after adding the fluctuating wind speeds.

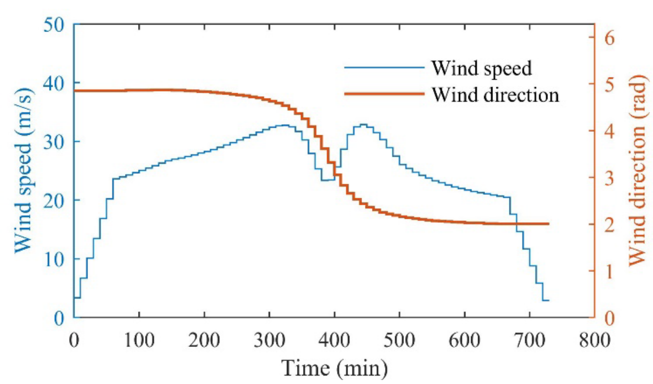

Fig. 3. An example of the 10-min mean wind speeds at 10 m height with the corresponding wind directions

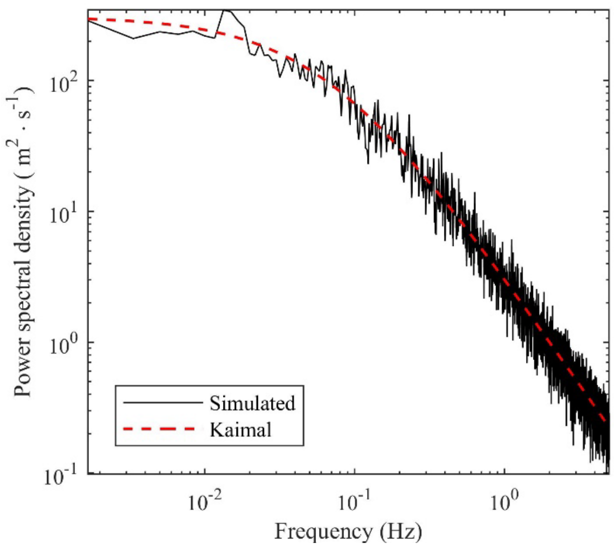

Fig. 4. Simulated and target spectra of fluctuating wind speeds

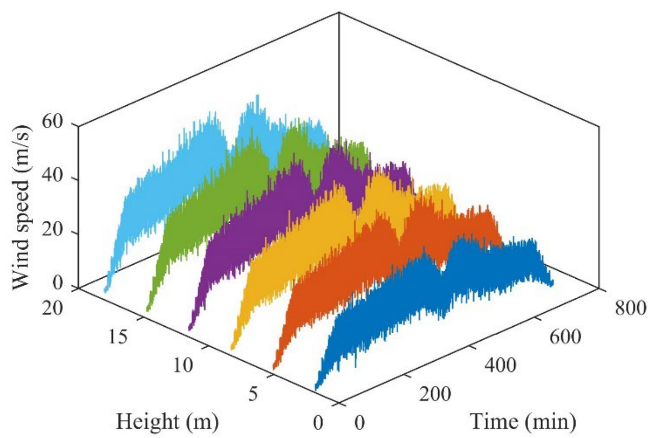

Fig. 5. Temporal-spatial evolution of synthetic hurricane wind speeds

3.2. Wind force calculation

Transmission towers are usually discretized into a series of panels along the height (see Fig. 6), with wind forces calculated for each panel separately [39]. For transmission towers subjected to yawed wind, ASCE 74 [29] gives the following equation for wind force calculation on a lattice panel

$$F_d = QK_zK_{zt}U_{3-sec}{}^2G_t(1+0.2\sin^2(2\Psi))\left(C_{ft}A_{mt}\cos^2\Psi + C_{fl}A_{ml}\sin^2\Psi\right) \tag{2}$$

where Q is the air density coefficient with a recommended value of 0.613 (m/s to Pa, converting wind speeds to pressure); K_z is the wind pressure exposure coefficient; K_{zt} is the topographic factor; G_t is the structure gust response factor; Ψ is the yaw angle as shown in Fig. 7; C_{ft} and C_{fl} are force coefficients associated with the face of the structure that is perpendicular to the transverse and longitudinal directions, respectively; and A_{mt} and A_{ml} are area of all members projected in the face of the structure that is perpendicular to the transverse and longitudinal directions, respectively. For conductors and ground wires subjected to yaw angles, ASCE 74 [29] gives the following equation for calculating wind forces perpendicular to the conductor or ground wire

$$F = QK_zK_{zt}U_{3-sec}{}^2G_wC_fA\cos^2\Psi \tag{3}$$

where G_w is the wire gust response factor; C_f is the force coefficient with a recommended value of 1.0; and A is the projected area of the wire (i.e., wind span times the diameter of the wire). As recommended by Mara [39], dynamic wind forces on the tower and wires are calculated using Eqs. (2) and (3) with the two terms $K_zK_{zt}U_{3-sec}{}^2G_t$ and $K_zK_{zt}U_{3-sec}{}^2G_w$ replaced by the simulated wind speeds at the corresponding height. As an example, Fig. 8 shows the calculated wind force time histories. Since the hurricane winds have time-variant wind directions, the wind forces are resolved into transvers and longitudinal directions for the ease to apply to the structure. Note that the two additional time histories in the transverse direction compared with those in the longitudinal direction are forces from one conductor and one ground wire.

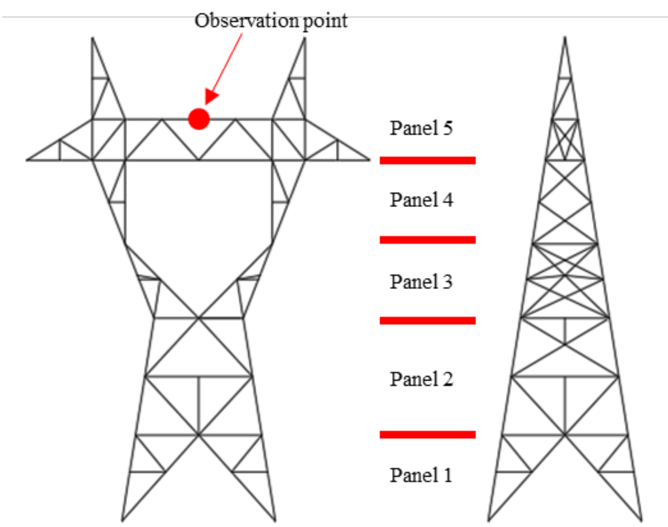

Fig. 6. An 18-m 115 kV transmission tower divided into panels

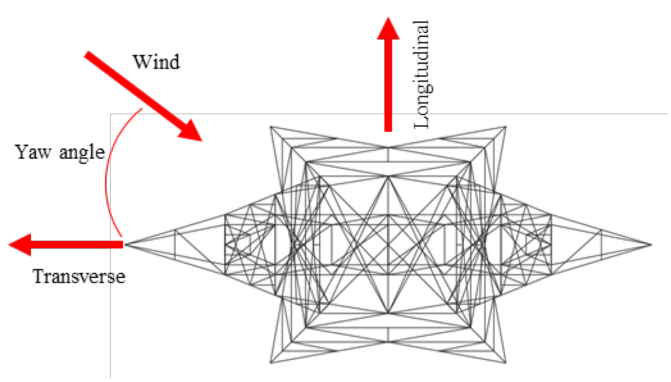

Fig. 7. Yawed wind on a transmission tower

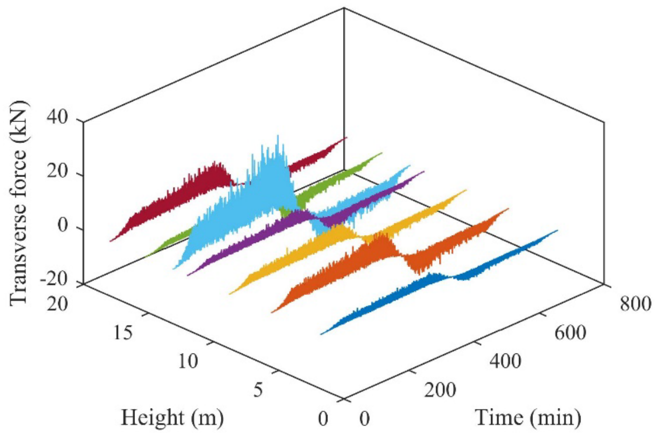

(a) Forces in the transverse direction

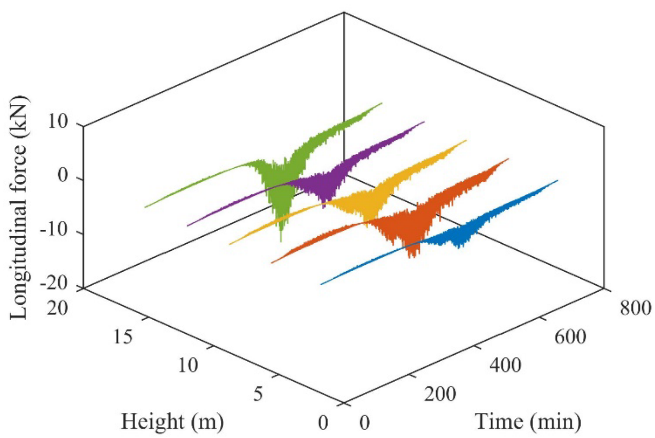

(b) Forces in the longitudinal direction

Fig. 8. Calculated wind forces on the transmission tower

4. Collapse fragility development

The event-based collapse fragility curves are developed in this section for transmission towers under hurricanes. First, the mathematical model for the event-based fragility is briefly introduced. This section then discussed the details of using IDA to capture collapse capacities of towers subjected to the hurricane wind records selected in Section 2. The parameters of fragility curves are then estimated from the data of collapse capacities using the method of moments or the maximum likelihood method. Nonlinear dynamic analysis is done using the OpenSees software [40] with the displacement-based beam element developed in Du and Hajjar [41] for modeling structures made of steel angles and tees such as the transmission towers, where both material and geometric nonlinearities are considered. The axial-flexural-torsional interaction behavior is modeled for steel angles because they may experience flexural-torsional buckling under complex loading conditions like combined axial forces and moments [42]. The Newmark-beta method is used for the integrator with a time step of 0.05 seconds as suggested by Mara [39] for transmission towers.

The uniaxial Steel01 material in OpenSees is adopted with the nominal yield stress. Residual stress is modeled explicitly by applying the residual stress pattern suggested by Kitipornchai and Lee [43] to fiber sections. Rayleigh damping is adopted with a 2% damping ratio. Other details of the finite element model in OpenSees can be found in Du and Hajjar [44]. The analyses for the IDAs were run on the DesignSafe cyberinfrastructure [45].

4.1. Event-based fragility and its parameter estimation

For the collapse limit state defined with a limit state function $g(\boldsymbol{X},\ \boldsymbol{Y}(0)\sim\boldsymbol{Y}(t))$, if the collapse capacity $IM_{collapse}$ is defined as the intensity measure associated with the onset of collapse for each sample of $\boldsymbol{Y}(t)$, the limit state function can be simplified as

$$g = IM_{collapse}\big(\boldsymbol{X}, \boldsymbol{Y}(0)\sim\boldsymbol{Y}(t)\big) - IM \tag{4}$$

Consequently, the fragility curve is the CDF of the random variable $IM_{collapse}$. This is because the conditional failure probability can be expressed as

$$P(g \leq 0|IM) = P\big(IM_{collapse} \leq IM\big|IM\big) \tag{5}$$

If it is assumed that $IM_{collapse}$ follows a lognormal distribution, then the fragility curve can be described as a lognormal CDF with two parameters, median θ and logarithmic standard deviation β. As used by many researchers [12, 16], the fragility is defined as

$$F(IM) = \Phi\left(\frac{\ln(IM/\theta)}{\beta}\right) \tag{6}$$

where Φ denotes the standard normal CDF. This fragility is designated as an event-based fragility because $IM_{collapse}$ is defined for a hurricane event and is obtained from IDA. This event-based fragility can only describe the failure probability after an event instead of at any time during the event.

Parameter estimation for the fragility curves involves estimating values of the model parameters θ and β using the simulated data of the collapse capacity. Here the estimates of parameters θ and β are denoted as $\hat{\theta}$ and $\hat{\beta}$, respectively. Two methods are widely used for estimating the two parameters of fragility curves. The method of moments assumes that the resulting distribution and the simulated data have the same moments. The maximum likelihood method assumes that the resulting distribution makes the simulated data most probable [46]. Choosing of the parameter estimation method depends on the characteristics of the simulated data. The method of moments requires data set of the collapse capacity $IM_{collapse}$, where parameters of fragility curves can be estimated from the simulated data by taking logarithms of each IDA curve's $IM_{collapse}$ value and calculating their mean and standard deviation [46, 47].

In addition to the traditional IDA, Baker [46] also proposed a truncated IDA method, which means conducting IDA only up to some intensity level IM_{max}. This truncated IDA is used due to some concerns of scaling ground motions to very large IM levels: first, it is computationally intensive; second, the portions of fragility curves at very large IM levels are of less interest; third, the accuracy of using scaled ground motions with extreme IM levels to model the real highly intensive hazards is still questionable [46]. Here, similar concerns are also present in this research on hurricanes. Therefore, the truncated IDA is also investigated in this paper, which means the hurricane wind records are scaled only up to a relatively large and reasonable intensity level. If all *n* hurricane wind records used to run IDA cause collapse before the maximum intensity level, then the method of moments can be adopted for parameter estimation. Otherwise, if there are only *m* records ($m < n$) that cause collapse, the method of moments is no longer suitable and instead the maximum likelihood method presented in Baker [46] is employed for parameter estimation. Specifically, the likelihood that the data set (*m* records cause collapse while (*n*-*m*) records does not) can be observed is shown as follows

$$Likelihood = \left[\prod_{i=1}^{m} \varphi\left(\frac{\ln(IM_{collapse,i}/\theta)}{\beta}\right)\right]\left[\prod_{j=1}^{n-m}\left(1-\Phi\left(\frac{\ln(IM_{max,j}/\theta)}{\beta}\right)\right)\right] \tag{7}$$

where $\varphi()$ is the probability density function of the standard normal distribution; $IM_{collapse,i}$ is the $IM_{collapse}$ value for the i^{th} IDA curve; $IM_{max,j}$ is the maximum intensity level after scaling of the j^{th} wind record in the (n - m) records that did not cause collapse. Here, $IM_{max,j}$ is used because different wind records may be scaled up to different intensity levels, which is discussed in detail in Section 4.2. The two parameters θ and β can be evaluated by maximizing the likelihood function in Eq. (7) through an optimization algorithm. It is easier to maximize the logarithm of the likelihood function with getting a mathematically equivalent result, so the parameters can be estimated through

$$\{\hat{\theta}, \hat{\beta}\} = \underset{\theta,\beta}{\operatorname{argmax}} \sum_{i=1}^{m}\left[\ln\varphi\left(\frac{\ln(IM_{collapse,i}/\theta)}{\beta}\right)\right] + \sum_{j=1}^{n-m}\left[\ln\left(1-\Phi\left(\frac{\ln(IM_{max,j}/\theta)}{\beta}\right)\right)\right] \tag{8}$$

4.2. Incremental dynamic analysis

In earthquake engineering, IDA is one common approach used to assess various limit states of structures, including global collapse capacity, where a suite of ground motions are scaled and applied to a structure in identifying the IM associated with the onset of collapse [27]. Recently, IDA was also applied to collapse capacity assessment of transmission towers under wind loading [39, 48]; however, the wind records used for IDA are not for storm events but only have 1-min or 5-min durations with a constant wind direction, which still have difficulties in dealing with the correlations of failure probabilities in different time intervals.

In this research, IDA is performed with a suite of hurricane wind records so that the results can be used for developing event-based fragilities. There are two main differences between IDA in wind engineering and earthquake engineering: one is the presence of mean and fluctuating wind speeds compared to the zero mean stochastic excitations of ground motions; another is the variation of the wind profile along the height of the structure [39]. To consider these differences, the 10-min mean wind speed records at 10 m height are first scaled for use in creating an IDA. The boundary layer model is then applied based on the scaled 10-min mean wind speed records at 10 m height to generate mean wind speeds at other heights, while the fluctuating wind speeds are generated and added to the mean wind speeds at different heights. For the scaling of ground motions, even though the efficient hunt-and-fill tracing algorithm [27] has been introduced in prior years, researchers often prefer the simpler but more expensive algorithm of scaling up ground motions by a constant IM increment [46]. Similarly, this work also uses a constant increment of the storm-maximum 10-min mean wind speed for the scaling of wind records. Note that the mean wind speed records instead of the final records including the fluctuating wind speeds are scaled. This is because the generated fluctuating wind speeds depend on the corresponding mean wind speeds at the same location considering that the spectrum and the coherence function of the fluctuating wind speeds are functions of the mean wind speeds. Scaling of the final wind records including the fluctuating wind speeds may invalidate the Kaimal spectrum and the coherence function of the fluctuating wind speeds. Thus, the IM (i.e., storm-maximum gust speed) increment is not exactly but close to being constant due to the randomness of the fluctuating wind speeds. This also explains why a record-dependent $IM_{max,j}$ instead of a constant IM_{max} appears in Eqs. (7) and (8). Each scaled record is applied to the tower for nonlinear dynamic analysis. An example of the applied wind speeds and structural responses is shown in Fig. 9, where the sampling frequency is 100 seconds.

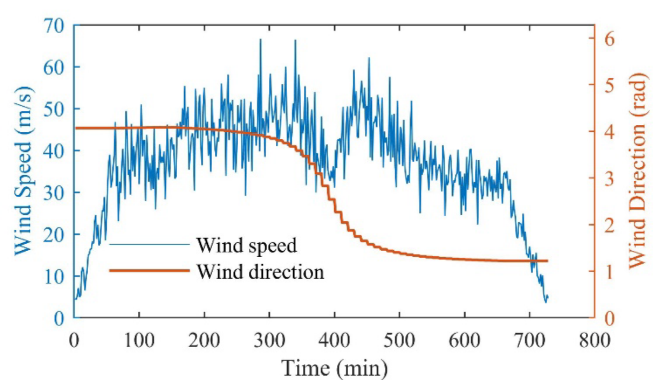

(a) Wind speeds and directions at 10 m height

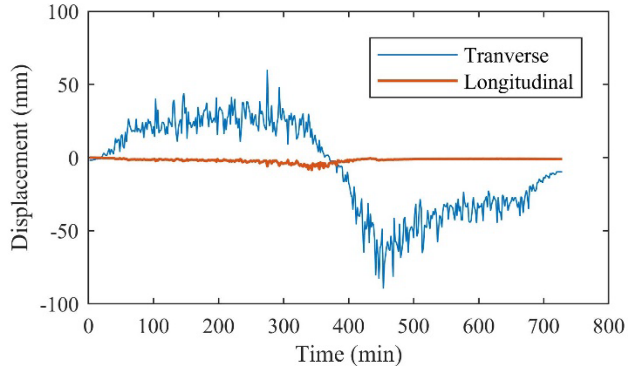

(b) Structural responses at the top of the tower

Fig. 9. Nonlinear dynamic analysis example

For transmission towers, the damage measure (DM) is chosen as the peak displacement at the top of the tower. An IDA curve is a plot of DM versus IM and Fig. 10 shows an example of the IDA curves using DM as the horizontal axis and IM as the vertical axis. To develop this IDA curve, the storm-maximum 10-min mean wind speed of a hurricane wind record is scaled to be 10 m/s to 55 m/s with a 5 m/s increment. A total of 10 nonlinear dynamic analyses were performed, but the one with the most intensive wind record did not converge and is omitted in the figure. Here the Piecewise Cubic Hermite Interpolating Polynomial (PCHIP) [49, 50] is employed to generate the IDA curve from the analysis points. Collapse is captured using the 20% slope criterion adapted from the IM-based rule in earthquake engineering [27]. As used in earthquake engineering, the onset of collapse is defined as the last point on the IDA curve with a tangent slope equal to 20% of the elastic slope (see the star in Fig. 10).

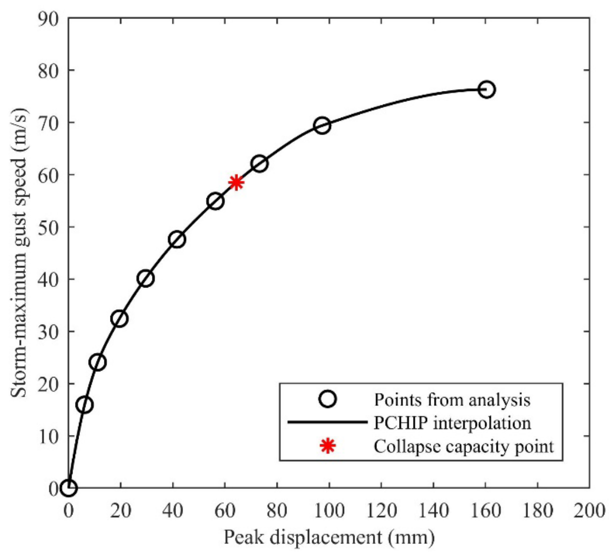

Fig. 10. An IDA curve generated using PCHIP interpolation and the corresponding collapse capacity point

Even though some prior work related to IDA recommends using spline interpolation to generate IDA curves [27, 51, 52], the authors found that spline interpolation is not a good option to capture the collapse capacity point with the 20% slope criterion for hurricane response. The spline interpolation conducts cubic interpolation to construct piecewise polynomials with continuous second-order derivatives, which can be prone to oscillations and overshoots between data points [53]. Therefore, the authors propose to use the shape-preserving piecewise cubic interpolation, PCHIP, which only has continuous first-order derivatives and has no overshoots and fewer oscillations if the data points are not smooth. Specifically, the PCHIP interpolant is monotonic for intervals where the original data is monotonic. To demonstrate the superiority of the PCHIP interpolation for generating IDA curves, Fig. 11 (a) and (b) compare the IDA curves and collapse capacity points obtained from the same dataset but with a different number of data points. Eleven data points are generated through IDA. It is seen that when using all 11 data points, the PCHIP interpolation produces almost the same collapse capacity point as using the first 9 data points, while the spline interpolation produces a different collapse capacity point. For the spline interpolation case, the polynomials fitted from 9 data points and those fitted from 11 data points have significant differences in their first derivatives. If collapse happens between points 8 and 9, points 10 and 11 should be unnecessary. This is also important for a truncated IDA in which fewer data points from analysis are intended to provide similar collapse capacity as a corresponding IDA having more data points, as discussed in Section 4.1.

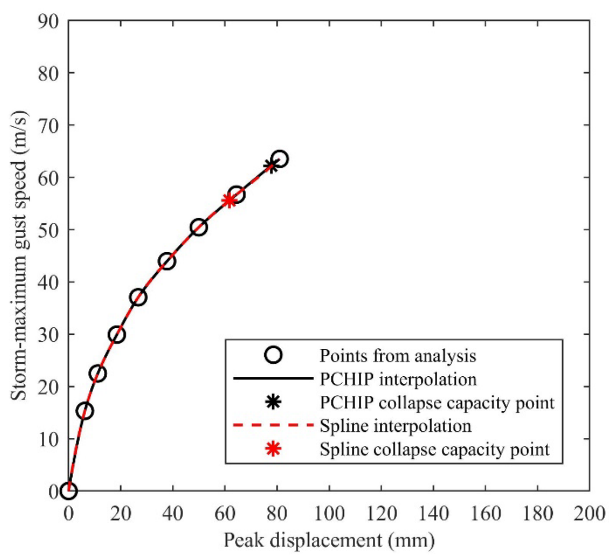

(a) Using 9 data points

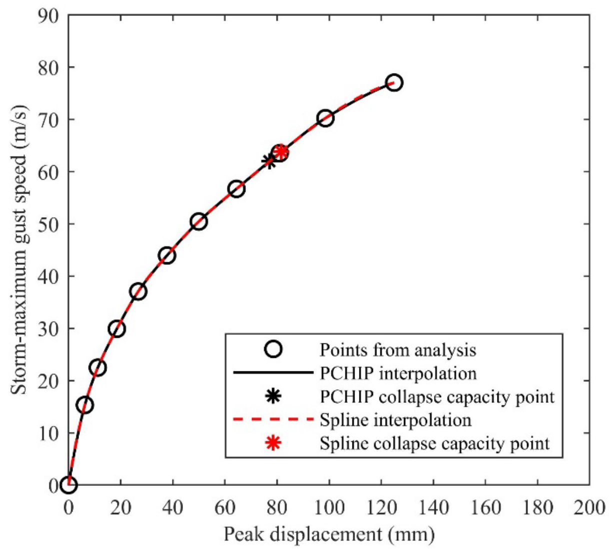

(b) Using 11 data points

Fig. 11. Comparison of the IDA curves and collapse capacity points from PCHIP and spline interpolations

4.3. Generation of fragility curves

To consider the uncertainties in hurricane wind speed and direction records, IDAs are run for a tower with a suite of wind records selected for the location of interest. If all wind records can produce collapse capacity values, then the method of moments is used for parameter estimation of fragility curves. On the contrary, if some of the records do not make the tower collapse until the maximum intensity level, they cannot produce collapse capacity values but can provide some lower bounds. This is designated a truncated IDA and the maximum likelihood method is used for parameter estimation. As an example, Fig. 12(a) illustrates 16 IDA curves with 16 collapse capacity points for the 115 kV tower shown in Fig. 6, while the corresponding fragility curve is developed using the method of moments. The result is shown in Fig. 12(b). Here the 16 hurricane wind records displayed in Fig. 2 are used and the storm-maximum 10-min mean wind speeds are scaled to be 10 m/s to 55 m/s with a 5 m/s increment. The nonconvergent computation results are not included in the figure. To demonstrate a truncated IDA, results from the highest two intensity levels are neglected for parameter estimation, which means the storm-maximum 10-min mean wind speed are scaled up to 45 m/s. Consequently, the 16 IDA curves can only produce 11 collapse capacity points as illustrated in Fig. 13(a). The corresponding fragility curve is estimated using the maximum likelihood method as in Eq. (8) and the result is shown in Fig. 13(b). It is seen that the truncated IDA can produce relatively accurate fragility curves with lower computational demand. Specifically, for this example the computational demand of a truncated IDA is 20% lower than a traditional IDA.

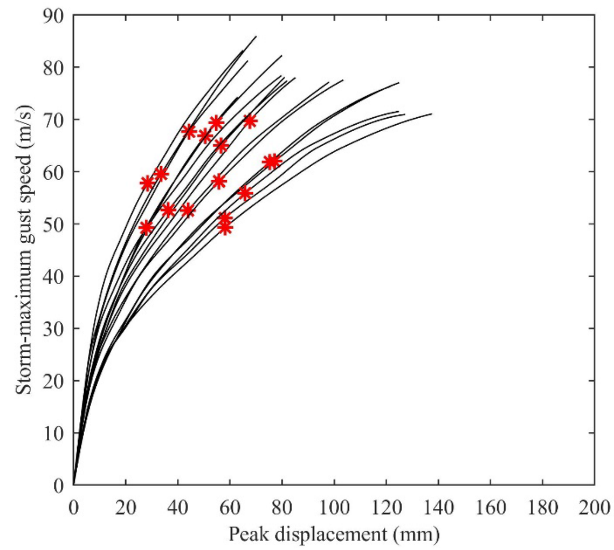

(a) IDA curves and the corresponding collapse capacity points (red stars)

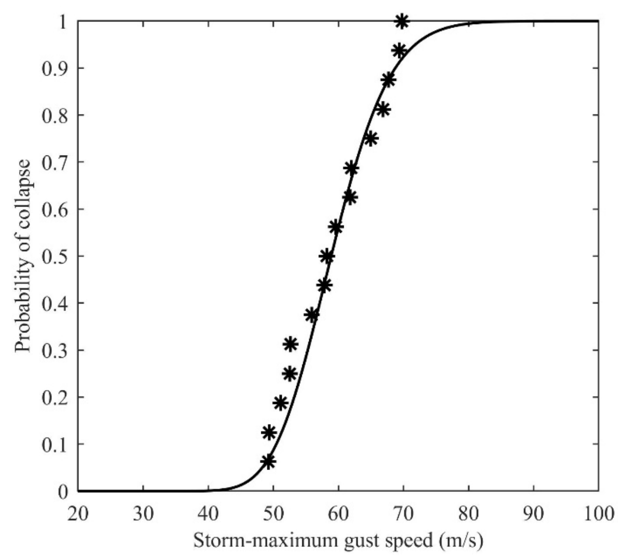

(b) Fragility curve estimated using the method of moment and the corresponding simulated data (black stars)

Fig. 12. Collapse fragility development using traditional IDA

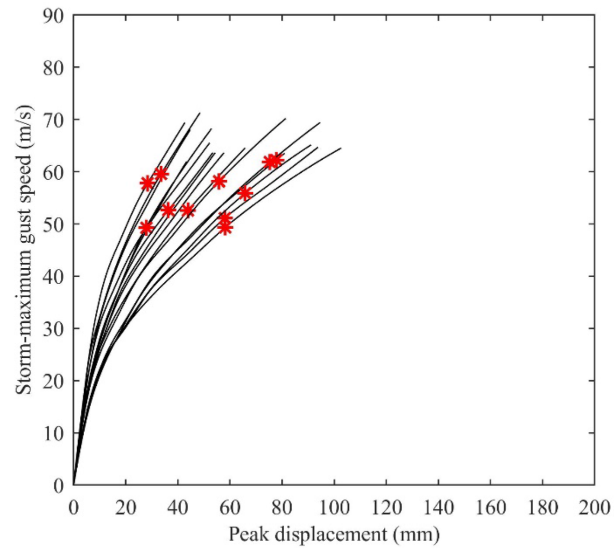

(a) IDA curves and the corresponding collapse capacity points (red stars)

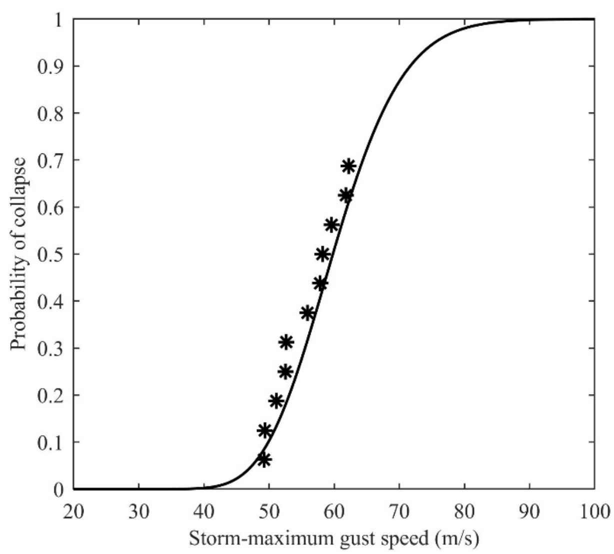

(b) Fragility curve estimated using the maximum likelihood method with the corresponding simulated data (black stars)

Fig. 13. Collapse fragility development using truncated IDA

The truncated IDA discussed earlier is due to the limit of the maximum intensity level. Sometimes an IDA may be truncated due to using a large increment of the intensity measure and the difficulty to converge the nonlinear dynamic analysis. If the analysis does not converge for some higher IM levels, the generated peak displacements for these IM levels should not be included in the IDA curve because they are not reliable. If the converged analyses with lower IM levels have not caused collapse, then this can be treated as a truncated IDA and all the nonconvergent analyses are ignored. Thus, the maximum likelihood method should be used for parameter estimation. For the j^{th} wind record, if the nonconvergent analysis starts from $IM_{k,j}$ in the k^{th}

increment of the scaled wind records, then the one step lower value $IM_{k-1,j}$ will be used to replace the $IM_{max,j}$ in Eqs. (7) and (8). Theoretically, more accurate results can be obtained by performing more nonlinear dynamic analyses with IM levels between $IM_{k-1,j}$ and $IM_{k,j}$; however, using the truncated IDA as discussed here can be an alternative way considering the computational intensity of IDAs. In addition, if one is confident that the nonconvergence of the time integration can represent dynamic collapse, then the smallest nonconvergent intensity measure $IM_{k,j}$ will be a upper bound of $IM_{collapse}$ and a better parameter estimation can be achieved by replacing the term $\left(1-\Phi\left(\frac{\ln(IM_{max,j}/\theta)}{\beta}\right)\right)$ in Eqs. (7) and (8) with this new term $\left(\Phi\left(\frac{\ln(IM_{k,j}/\theta)}{\beta}\right)-\Phi\left(\frac{\ln(IM_{k-1,j}/\theta)}{\beta}\right)\right)$; however, this is not done in this work. These equations can be modified if within the development of a fragility curve some IDAs are truncated due to the limit of the maximum intensity level while some other IDAs are truncated due to nonconvergence.

5. Fragility development for a region

Fragility curves of transmission towers are essential for fast regional damage assessment of electrical transmission networks. Given the fact that characteristics of hurricane wind records are site-specific, fragility curves may be developed for towers at different locations. To demonstrate this idea, the geographic information of 115 kV overhead transmission lines in Massachusetts is collected from HIFLD open data [54] and shown in Fig. 14. The same grids in Fig. 1 for hurricane wind records selection are used here to assign the transmission towers along the lines to their corresponding grids. In addition, since transmission towers are not axisymmetric, the orientation of a tower also has significant impacts on its collapse capacity and fragility curve. Theoretically, the orientation of towers can be obtained from the geographic data of transmission lines; however, developing fragility curves for all existing orientations is intractable due to the huge amount of computational demand. Thus, in this research towers are assumed to be doubly symmetric and fragility curves are only developed for five orientations, which are 0, π/8, π/4, 3π/8, and π/2. These orientations are clockwise positive from the North direction. Considering that the detailed information of towers is not publicly available, all towers in this 115 kV network are assumed to be the same as the one shown in Fig. 6, which may be unreasonable for practical applications but can be accepted here for a demonstration of the proposed methodology. To summarize, five fragility curves are developed for the 115 kV towers in each grid, and the selected hurricane wind records for each grid are employed to run IDAs. As an example, Fig. 15 plots fragility curves for the 115 kV towers with different orientations in two different grids, where the differences between the fragility curves in these two grids are due to the site-specific hurricane wind records. When using the fragility curves, the location and orientation of a tower should be determined first. An appropriate fragility curve may then be chosen from the developed fragility dataset. Since only five orientations are considered here, users can choose the fragility curve whose orientation is closest to the real orientation of the tower or apply interpolation techniques. The procedure described in this section is only a methodology, since the towers are only representative and cannot be used directly to assess the region of interest. Although only 115 kV transmission lines in Massachusetts are studied here, fragility curves of towers with other voltage levels can be developed using the same methodology.

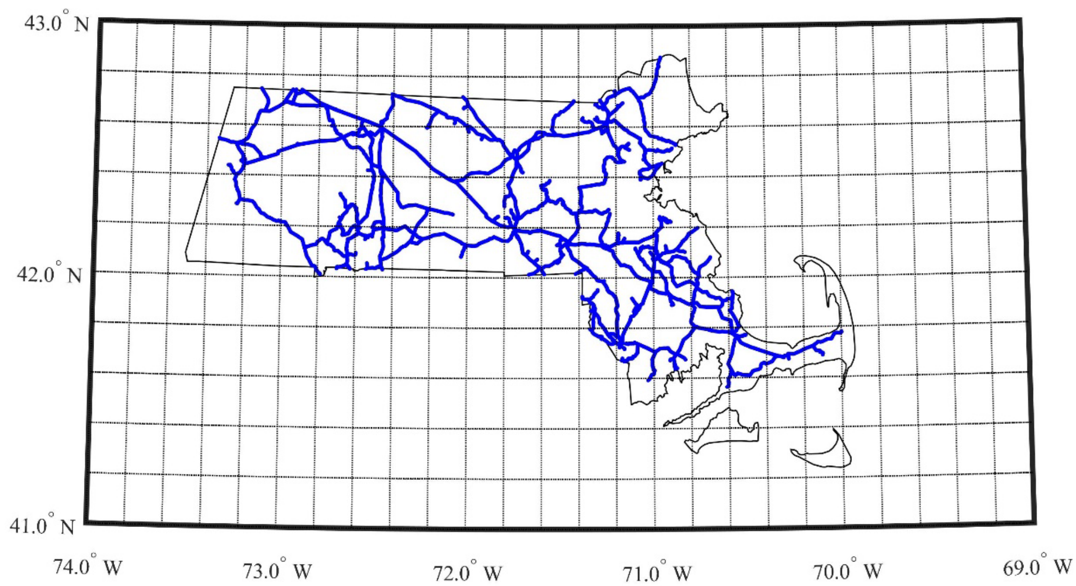

Fig. 14. Geographic information of 115 kV overhead transmission lines in Massachusetts

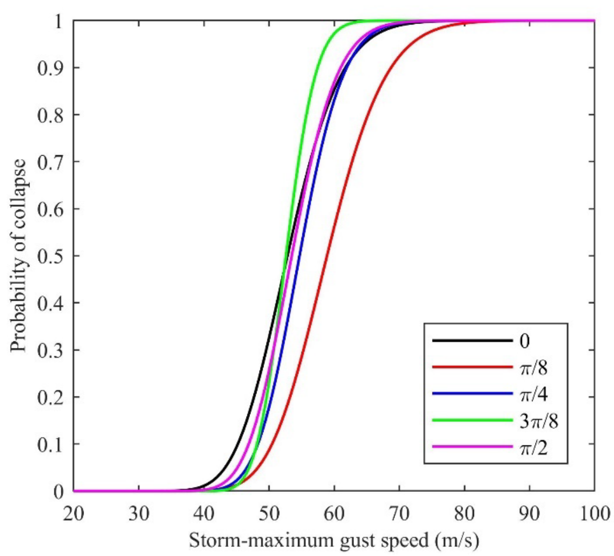

(a) Grid 86 with a centroid of latitude 41.7 and longitude -70.1

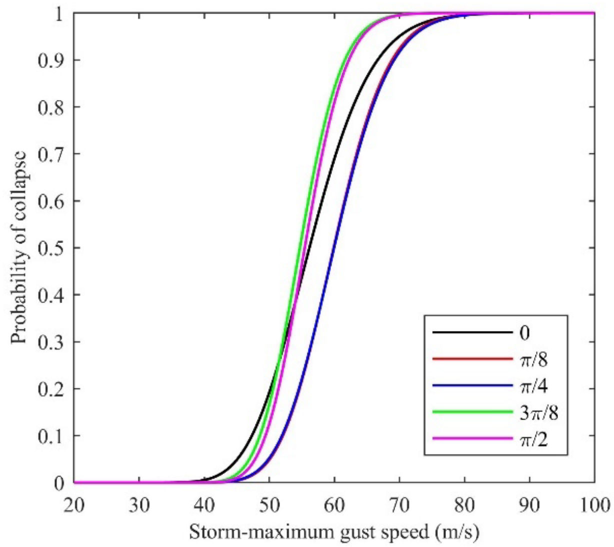

(b) Grid 78 with a centroid of latitude 41.7 and longitude -70.5

Fig. 15. Fragility curves for 115 kV towers with different orientations in two grids

6. Conclusions

This paper presents a methodology for developing event-based collapse fragility curves for electrical transmission towers subjected to hurricanes. The event-based fragility curve describes the collapse probability of a structure after a hurricane event. Uncertainties in hurricane wind speed, direction, and duration are accounted for by assessing collapse capacities of transmission towers with a suite of hurricane wind records for a specific location. Both traditional IDA and truncated IDA are introduced to capture the collapse capacities with scaling of the hurricane wind records. The method of moments and the maximum likelihood method are adopted for parameter estimation of fragility curves based on the collapse capacity data obtained from IDA. Finally, a procedure for developing a set of fragility curves for a region is proposed and demonstrated with considerations of site-specific hurricane wind records and tower orientations. The methodology presented in this work can help in performing a comprehensive damage assessment of electrical transmission networks.

Acknowledgement

The material presented in this paper is based upon work supported by National Science Foundation under Grant No. CRISP-1638234, the American Institute of Steel Construction, the American Iron and Steel Institute, the Metal Building Manufacturers Association, the Steel Deck Institute, the Steel Joist Institute, and Northeastern University. This support is gratefully acknowledged. This work used computational resources provided by the Natural Hazards Engineering Research Infrastructure: Cyberinfrastructure

(DesignSafe), which is supported by National Science Foundation Grant No. CMMI-2022469. The authors wish to thank Dr. Weichiang Pang at Clemson University for providing the synthetic hurricane catalog.

References

[1] Cauffman SA, Phan LT, Sadek F, Fritz WP, Duthinh D, Rossiter Jr WJ. Performance of physical structures in Hurricane Katrina and Hurricane Rita: A reconnaissance report (NIST TN 1476). 2006.

[2] Coporation NAER. Hurrican Harvey Event Analysis Report. Atlanta, GA 30326: North Amereican Electric Reliability Coporation; 2018.

[3] Dunn S, Wilkinson S, Alderson D, Fowler H, Galasso C. Fragility curves for assessing the resilience of electricity networks constructed from an extensive fault database. Natural Hazards Review. 2017;19:04017019.

[4] Ouyang M, Duenas-Osorio L. Multi-dimensional hurricane resilience assessment of electric power systems. Structural Safety. 2014;48:15-24.

[5] Cai Y, Xie Q, Xue S, Hu L, Kareem A. Fragility modelling framework for transmission line towers under winds. Engineering Structures. 2019;191:686-97.

[6] Fu X, Li H-N, Li G. Fragility analysis and estimation of collapse status for transmission tower subjected to wind and rain loads. Structural safety. 2016;58:1-10.

[7] Fu X, Li H-N, Li G, Dong Z-Q. Fragility analysis of a transmission tower under combined wind and rain loads. Journal of Wind Engineering and Industrial Aerodynamics. 2020;199:104098.

[8] Ma L, Khazaali M, Bocchini P. Component-based fragility analysis of transmission towers subjected to hurricane wind load. Engineering Structures. 2021;242:112586.

[9] Darestani YM, Jeddi AB, Shafieezadeh A. Hurricane Fragility Assessment of Power Transmission Towers for a New Set of Performance-Based Limit States. Engineering for Extremes: Springer; 2022. p. 167-88.

[10] Tian L, Zhang X, Fu X. Fragility analysis of a long-span transmission tower–line system under wind loads. Advances in Structural Engineering. 2020;23:2110-20.

[11] ASCE. Prestandard for Performance-Based Wind Design. Reston, VA: American Society of Civil Engineers; 2019.

[12] Ellingwood BR, Rosowsky DV, Li Y, Kim JH. Fragility assessment of light-frame wood construction subjected to wind and earthquake hazards. Journal of Structural Engineering. 2004;130:1921-30.

[13] Li Y. Fragility methodology for performance-based engineering of wood-frame residential construction [PhD Dissertation]. Atlanta, GA: Georgia Institute of Technology; 2005.

[14] Li Y, Ellingwood BR. Hurricane damage to residential construction in the US: Importance of uncertainty modeling in risk assessment. Engineering structures. 2006;28:1009-18.

[15] Shanmugam B. Probablistic assessment of roof uplift capacities in low-rise residential construction [PhD Dissertation]. Clemson, South Carolina, USA: Clemson University; 2011.

[16] Shinozuka M, Feng MQ, Lee J, Naganuma T. Statistical analysis of fragility curves. Journal of engineering mechanics. 2000;126:1224-31.

[17] Shafieezadeh A, Onyewuchi UP, Begovic MM, DesRoches R. Age-dependent fragility models of utility wood poles in power distribution networks against extreme wind hazards. IEEE Transactions on Power Delivery. 2013;29:131-9.

[18] ASCE. Minimum Design Loads for Buildings and Other Structures (ASCE Standard 7-10). Reston, VA: American Society of Civil Engineers; 2010.

[19] ASCE. Minimum Design Loads and associated criteria for Buildings and Other Structures (ASCE Standard 7-16). Reston, VA: American Society of Civil Engineers; 2016.

[20] Der Kiureghian A. First-and second-order reliability methods. In: E. Nikolaidis, D. Ghiocel, Singhal S, editors. Engineering design reliability handbook. Boca Raton, FL: CRC Press; 2005.

[21] Kim S-M, Ok S-Y, Song J. Multi-scale dynamic system reliability analysis of actively-controlled structures under random stationary ground motions. KSCE Journal of Civil Engineering. 2019;23:1259-70.

[22] Kim D-S, Ok S-Y, Song J, Koh H-M. System reliability analysis using dominant failure modes identified by selective searching technique. Reliability Engineering & System Safety. 2013;119:316-31.

[23] Song J, Ok SY. Multi‐scale system reliability analysis of lifeline networks under earthquake hazards. Earthquake engineering & structural dynamics. 2010;39:259-79.

[24] Straub D, Schneider R, Bismut E, Kim H-J. Reliability analysis of deteriorating structural systems. Structural safety. 2020;82:101877.

[25] Hallowell ST, Myers AT, Arwade SR, Pang W, Rawal P, Hines EM et al. Hurricane risk assessment of offshore wind turbines. Renewable Energy. 2018;125:234-49.

[26] Du X, Hajjar JF, Bond RB, Ren P, Sun H. Clustering and selection of hurricane wind records using a machine learning approach. Engineering Archive. 2022.

[27] Vamvatsikos D, Cornell CA. Incremental dynamic analysis. Earthquake Engineering & Structural Dynamics. 2002;31:491-514.

[28] Liu F. Projections of future US design wind speeds and hurricane losses due to climate change [PhD Dissertation]. Clemson, SC: Clemson University; 2014.

[29] ASCE. Guidelines for electrical transmission line structural loading. Reston, VA: American Society of Civil Engineers; 2020.

[30] Simiu E, Patel V, Nash J. Mean wind profiles in hurricanes. JOURNAL OF ENINEERING MECHANICS DVISION ASCE. 1974;100:833-7.

[31] Simiu E, Scanlan RH. Wind effects on structures: fundamentals and applications to design. 3rd ed. New York, NY: John Wiley & Sons, Inc.; 1996.

[32] Simiu E, Patel V, Nash JF. Mean speed profiles of hurricane winds. Journal of the Engineering Mechanics Division. 1976;102:265-73.

[33] Kaimal JC, Wyngaard J, Izumi Y, Coté O. Spectral characteristics of surface‐layer turbulence. Quarterly Journal of the Royal Meteorological Society. 1972;98:563-89.

[34] Deodatis G. Simulation of ergodic multivariate stochastic processes. Journal of engineering mechanics. 1996;122:778-87.

[35] Shinozuka M. Monte Carlo solution of structural dynamics. Computers & Structures. 1972;2:855-74.

[36] Shinozuka M, Jan C-M. Digital simulation of random processes and its applications. Journal of sound and vibration. 1972;25:111-28.

[37] Davenport AG. The spectrum of horizontal gustiness near the ground in high winds. Quarterly Journal of the Royal Meteorological Society. 1961;87:194-211.

[38] Cheynet E. Wind field simulation (the user-friendly version). GitHub; 2020.

[39] Mara TG. Capacity assessment of a transmission tower under wind loading [PhD Dissertation]. London, Ontario, Canada: The University of Western Ontario; 2013.

[40] McKenna F, Scott MH, Fenves GL. Nonlinear finite-element analysis software architecture using object composition. Journal of Computing in Civil Engineering. 2010;24:95-107.

[41] Du X, Hajjar JF. Three-dimensional nonlinear displacement-based beam element for members with angle and tee sections. Engineering Structures. 2021;239:112239.

[42] Liu Y, Hui L. Experimental study of beam–column behaviour of steel single angles. Journal of Constructional Steel Research. 2008;64:505-14.

[43] Kitipornchai S, Lee H. Inelastic buckling of single-angle, tee and double-angle struts. Journal of Constructional Steel Research. 1986;6:3-20.

[44] Du X, Hajjar JF. Hurricane fragility analysis of electrical transmission towers. The Electrical Transmission and Substation Structures Conference. Orlando, FL: American Society of Civil Engineers; 2022.

[45] Rathje EM, Dawson C, Padgett JE, Pinelli J-P, Stanzione D, Adair A et al. DesignSafe: New cyberinfrastructure for natural hazards engineering. Natural Hazards Review. 2017;18:06017001.
[46] Baker JW. Efficient analytical fragility function fitting using dynamic structural analysis. Earthquake Spectra. 2015;31:579-99.
[47] Ibarra LF, Krawinkler H. Global collapse of frame structures under seismic excitations. Stanford, CA: John A. Blume Earthquake Engineering Center; 2005.
[48] Banik S, Hong H, Kopp GA. Assessment of capacity curves for transmission line towers under wind loading. Wind & structures. 2010;13:1-20.
[49] Fritsch FN, Carlson RE. Monotone piecewise cubic interpolation. SIAM Journal on Numerical Analysis. 1980;17:238-46.
[50] Kahaner D, Moler C, Nash S. Numerical methods and software: Prentice-Hall, Inc.; 1989.
[51] Vamvatsikos D, Cornell CA. Applied incremental dynamic analysis. Earthquake spectra. 2004;20:523-53.
[52] Vamvatsikos D, Jalayer F, Cornell CA. Application of incremental dynamic analysis to an RC-structure. Proceedings of the FIB symposium on concrete structures in seismic regions2003. p. 75-86.
[53] MathWorks. MATLAB Documentation. 2022.
[54] HIFLD. Homeland Infrastructure Foundation-Level Data (HIFLD). U.S. Department of Homeland Security; 2018.